

FACILE HYDROTHERMAL SYNTHESIS OF Pd, Ir, Pd-Ir PARTICLES ON CMK-3 FOR REDUCTIVE CATALYTIC FRACTIONATION OF BIRCH WOOD

ALEKSANDR S. KAZACHENKO,^{*, **, ***, ****} ROMAN V. BORISOV,^{**, ***}
 ANGELINA V. MIROSHNIKOVA,^{**, ***} OLEG V. BELOUSOV,^{**, ***} SERGEY V. BARISHNIKOV,^{***}
 ANDREY M. SKRIPNIKOV,^{**, ***} OLGA S. SELEZNEVA,^{***}
 MAXIM N. LIKHATSKI^{***} and ANATOLY M. ZHIZHAEV^{***}

**Reshetnev Siberian State University of Science and Technology, Institute of Chemical Technologies, Pr. Mira 82, Krasnoyarsk, Russia*

***Siberian Federal University, Pr. Svobodny 79, 660041 Krasnoyarsk, Russia*

****Institute of Chemistry and Chemical Technology, Krasnoyarsk Science Center, Siberian Branch, Russian Academy of Sciences, Akademgorodok 50/24, 660036 Krasnoyarsk, Russia*

*****Prof. V.F. Voino-Yasenetsky Krasnoyarsk State Medical University of the Ministry of Healthcare of the Russian Federation, Str. Partizan Zheleznyak, bld. 1, 660022 Krasnoyarsk, Russia*

✉ Corresponding author: A. S. Kazachenko, leo_lion_leo@mail.ru

Received April 22, 2025

Palladium, iridium and iridium-palladium particles were applied to ordered mesoporous carbon material CMK-3 by a simple hydrothermal method. Iridium particles with a diameter of 3-6 nm were formed on the carbon material upon reduction from aqueous solutions of potassium hexachloroiridate(IV) by sodium tetrahydroborate in alkaline media at a temperature of 180 °C. Palladium particles had a wide size distribution from 3 to 40 nm and were obtained by decomposition of an alkaline solution of tetraamminepalladium(II) chloride in an autoclave. The corresponding reflections of metal phases were detected by X-ray phase analysis. The proportion of metallic Ir and Pd on the surface was determined by X-ray photoelectron spectroscopy and amounted to 25% and 75%, respectively. After bombardment with argon ions for 1 minute, the surface fraction of iridium was more than 50%, and that of palladium was more than 90%. The obtained catalysts were used in the process of reductive catalytic fractionation (RCF) of birch wood, which allowed to effectively separate lignocellulosic biomass into valuable chemical products. The use of catalysts based on Pd and Pd-Ir led to a significant increase in the yield of liquid products (up to 58.6% by weight) and a decrease in the lignin content in the solid residue (up to 6.0% by weight). The highest wood conversion (60.7% by weight) was achieved using the Pd/CMK-3 catalyst. The results of the work demonstrate the prospects for using the synthesized catalysts for sustainable processing of biomass into valuable chemical products.

Keywords: iridium, palladium, hydrothermal synthesis, mesoporous carbon material, catalysts, RCF

INTRODUCTION

Iridium nanoparticles applied to various matrices exhibit high catalytic activity in hydrogenation, dehydrogenation, oxygen extraction and reduction processes, and in water electrolyzers.¹⁻⁶ A review of the latest advances in the use of iridium-containing catalysts in hydrogenation processes is given in a monograph by Martínez-Prieto *et al.*⁷ Iridium nanoparticles, among platinum group metals, are characterized by high activity, selectivity, and the highest resistance to oxidation in air. Improving the catalyst characteristics can be achieved by introducing a second metal, such as palladium.⁸⁻¹² Palladium-

based catalysts exhibit high activity in hydrogenation processes.^{13,14} Highly porous carbon materials, such as sibunit, graphene, nanotubes, and CMK-3,¹⁵⁻¹⁸ are widely used as metal carriers. Carbon substrates have a number of advantages: chemical and thermal stability over a wide temperature range and the possibility of synthesis with a high degree of purity.

The use of mesoporous and mesostructured carbon materials, such as CMK-3, opens up wide possibilities for catalysis due to the highly ordered porosity of the support.¹⁹ The size and volume of pores, as well as the specific surface area of

mesostructured materials, can be tuned by changing the porous structure of silicon templates (e.g., SBA-15).^{20,21} Despite the huge number of methods for obtaining platinum group metal nanoparticles on various supports, the most widely used are methods of chemical reduction of complex compounds. In this case, an increase in temperature favors the rapid formation of numerous nuclei of a new phase, and thus smaller nanoparticles are obtained.²² Therefore, it is promising to obtain platinum group metal nanoparticles on a support by chemical reduction of complex compounds under hydrothermal conditions. The processes of formation of mono- and bimetallic nanoparticles of non-ferrous and noble metals on oxide and carbon supports in autoclaves at temperatures above 110 °C are considered in previous works.^{17,23-25}

Reductive catalytic fractionation (RCF) of plant biomass has become a promising strategy for the sustainable processing of lignocellulosic materials.²⁶ This process is aimed at the efficient decomposition of biomass into valuable platform chemicals, fuels and materials, minimizing waste and energy consumption. RCF has attracted considerable attention in recent years due to its potential to solve problems associated with traditional biomass processing methods, such as harsh reaction conditions, low selectivity and low yields of target products.²⁷ RCF typically involves the depolymerization of lignin and hemicelluloses, followed by catalytic hydrogenation or hydrogenolysis of the resulting fragments.²⁸ The process is often carried out in the presence of a solvent (e.g. methanol, ethanol or other alcohols) and a catalyst (e.g. supported metal catalysts, such as Pd, Ru or Ni).²⁹ The key advantage of RCF is its ability to simultaneously decompose lignin into aromatic monomers and oligomers, while preserving the carbohydrate fraction (cellulose) for further processing.³⁰

The aim of this work is to synthesize and characterize Pd, Ir, Pd-Ir nanoparticles on the mesoporous carbon material CMK-3 and to study the resulting catalysts in the process of reductive catalytic fractionation of birch wood.

EXPERIMENTAL

Materials and synthesis procedures

All reagents used in this work were of analytical grade. The following were used in the work: potassium hexachloroiridate(IV) and tetraamminepalladium(II) chloride obtained according to a previously described procedure³¹ from commercial reagents (OAO

Krasnotsvetmet); hydrochloric acid, sodium tetrahydridoborate, sodium hydroxide, aqueous ammonia, and deionized water prepared using the Direct-Q3 water purification system (Millipore, USA).

The synthesis of CMK-3 was carried out by a previously published procedure,¹⁷ by means of double impregnation of the SBA-15 silicate matrix with a sucrose solution, followed by high-temperature carbonization in an inert atmosphere. After this, the silicate matrix was dissolved in alkalis.^{17,20} The deposition of platinum metals was carried out on CMK-3, which was pre-treated in an alkaline (0.05 M KOH) medium at a temperature of 180 °C for 60 minutes to remove residual silicon. The synthesis was carried out in titanium autoclaves with fluoroplastic liners with a volume of 32 cm³, the design of which has been described previously.^{31,32}

To apply Ir, a weighed portion of CMK-3 (1 g) was placed in the autoclave, 10.0 cm³ of a solution of potassium hexachloroiridate (IV), prepared by dissolving the required weighed portion of the salt in distilled water, and 10.0 mL of a 1 M KOH solution were added. A weighed portion of sodium tetrahydridoborate was placed in a fluoroplastic cup on the inner surface of the autoclave lid. The autoclave was sealed and heated in an air thermostat in a vertical position for 40 min to 180 °C. After heating, stirring was turned on, ensuring mixing of the phases. After 15 minutes, the autoclave was cooled with running water and opened, the solution was filtered to determine the concentration of iridium. The precipitate, in the form of a black powder, was repeatedly washed with hot distilled water.

The solid phase was precipitated in a CR4000 centrifuge (Centurion Scientific, UK) for 15 min at 4000 rpm. The precipitates were dried to constant weight under vacuum at a temperature of 80 °C. To apply palladium, a weighed portion of the CMK-3 material or the previously obtained Ir/CMK-3 material was placed in a fluoroplastic reactor, a specified amount of tetraamminepalladium (II) chloride was added, 20 cm³ of 0.05 M KOH solution was poured in, and the system was sealed. Stirring was carried out for 15 minutes at 25 °C, after which the autoclave was placed in a thermostat heated to 180 °C for 120 minutes with constant rotation in the vertical plane. After the experiment, the autoclave was opened, the solution was taken for analysis, and the solid phase was repeatedly washed with hot distilled water and dried at 80 °C under vacuum.

Characterization

Low-temperature nitrogen adsorption isotherms for the studied materials were recorded using an ASAP-2420 analyzer (Micromeritics, USA) at 77K. Texture characteristics were calculated using the BJH and BET methods. The specific surface area of the material after alkaline treatment and washing with distilled water was 945 m²/g, the pore volume was 1.28 cm³/g with an average pore diameter of 5.4 nm. X-ray powder

diffraction patterns were acquired from the air-dried reaction products using an X'Pert Pro (Panalytical, Netherlands) diffractometer with Cu K α radiation ($\lambda = 0.15418$ nm) in a 2 θ angle range of 5° to 80° with a step of 0.02°.

The morphological features of the deposited particles were studied by scanning electron microscopy on an S5500 (Hitachi, Japan) and a TM4000Plus (Hitachi, Japan) scanning electron microscopes with a Quantax 150 microanalysis system (Bruker, Germany).

Transmission electron microscopy (TEM) images were acquired from ground samples using an HT7700 instrument (Hitachi, Japan) operated at 200 kV. For the TEM experiment, the particles were dispersed in ethanol, and then a droplet of the suspension was placed on a carbon-coated grid and allowed to dry at room temperature.

X-ray photoelectron spectra were acquired with a SPECS instrument (SPECS, Germany) equipped with a Phoibos 150 MCD-9 analyzer operated at the pass energy of 20 eV for survey spectra and 10 eV for high-resolution spectra. Monochromatized Al K α irradiation (1486.7 eV) was used as an excitation source. The high-resolution spectra were fitted with Doniach-Sunjic peak profiles for Pd 3d regions or with Gaussian-Lorentzian ones for Ir 4f bands after subtraction of the Shirley-type background using the CasaXPS software package ver.2.3.15. The binding energy scale was charge-corrected using the C 1s line of the adventitious aliphatic carbon (285.0 eV).

Atomic concentrations of elements were calculated from the survey spectra. The content of chemical elements in solutions was determined by inductively coupled plasma mass spectrometry on an Agilent 7900 instrument (Agilent, USA).

Hydrogenation of birch wood

The hydrogenation process was carried out in a ChemRe SYstem R-201 autoclave (Korea) with a volume of 300 mL. The reactor was loaded with 60 mL of ethanol, 3.0 g of substrate and 0.3 g of catalyst. Then, the autoclave was hermetically sealed and purged with argon to remove air. Hydrogen was supplied, the initial pressure of which was 4 MPa. The reaction was carried out with constant stirring at a speed of 1000 rpm at a temperature of 250 °C for 3 hours. The rate of temperature rise was 10 °C/min, the time to reach the required temperature was 20-25 minutes. The operating pressure in the reactor was 10.0 MPa. After cooling the reaction mixture to room temperature, the gaseous products were collected in a gasometer, their volume was measured, and the composition was determined by gas chromatography. Then, the reaction products were quantitatively discharged from the autoclave by washing with ethanol, and the resulting mixture of liquid and solid products was separated by filtration.

The solid was washed with ethanol until the solvent became colorless. The solvent was removed from the liquid product using a rotary evaporator, and the product

was brought to constant weight by drying under vacuum (1 mm Hg) at room temperature. The yield of liquid products (α_1), the yield of solid product (α_2), the total yield of gaseous products (α_3) and wood conversion (χ_d) were determined using formulas (1-4):

$$\alpha_1 = \frac{m_l(g)}{m_{in}(g)} \times 100\% \quad (1)$$

$$\alpha_2 = \frac{m_s(g) - m_{cat}(g)}{m_{in}(g)} \times 100\% \quad (2)$$

$$\alpha_3 = \frac{m_g(g)}{m_{in}(g)} \times 100\% \quad (3)$$

$$\chi_d = \frac{m_{in}(g) + m_{cat}(g) - m_s(g)}{m_{in}(g)} \times 100\% \quad (4)$$

where m_l – mass of liquid products (g), m_{in} – mass of the initial sample (g), m_s – mass of the solid residue (g), m_{cat} – mass of the catalyst (g), m_g – mass of gaseous products (g).

Study of birch wood hydrogenation products

The composition of gaseous products of birch wood in supercritical ethanol was determined by GC using a Kristall 2000 M chromatograph (Chromatek, Russia) with a thermal conductivity detector. Carrier gas was helium (flow rate: 15 mL/min), and detector temperature was 170 °C. To analyze CO and CH₄, a column with NaX zeolite (3 m × 2 mm) was used in isothermal mode at a temperature of 60 °C. Analysis of CO₂ and hydrocarbon gases was carried out on a column with Porapak Q in the following mode: 1 min – 60 °C and then increasing the temperature to 180 °C at a rate of 10 °C/min.

The solid product of hydrogenation of birch wood was analyzed for the content of hemicelluloses, cellulose and lignin. The content of residual lignin in the solid product was determined using hydrolysis with 72% sulfuric acid according to the Komarov method,³⁴ and the content of hemicelluloses was determined by gas chromatography (GC) of the resulting hydrolysates.³⁵ The content and composition of monosaccharides in hydrolysates were determined by GC using a Varian-450 GC gas chromatograph with a flame ionization detector and a VF-624ms capillary column with a length of 30 m and an internal diameter of 0.32 mm. Chromatography conditions: helium carrier gas, injector temperature 250 °C, initial column temperature 50 °C (5 min), temperature increase to 180 °C at a rate of 10 °C/min, holding the temperature at 180 °C for 37 minutes. Before analysis, the hydrolyzate was derivatized according to an earlier described procedure,³ to obtain trimethylsilyl derivatives. Sorbitol was used as an internal standard. Peaks were identified by the retention time of tautomeric forms of monosaccharides. Cellulose was determined in the solid products of flaxseed hydrogenation using the nitrogen-alcohol method (Kürschner-Hoffer).³⁴

Liquid ethanol-soluble products of non-catalytic and catalytic hydrogenation of birch wood were analyzed by GC-MS using an Agilent 7890A chromatograph equipped with an Agilent 7000A Triple Quad selective mass detector, recording the total ion current. Product

separation was carried out on an HP-5MS capillary column with temperature programming in the range of 40–250 °C. Identification was carried out using the NIST MS Search 2.0 instrument database. To quantify the yield of monomeric compounds, standard substances, such as guaiacol, syringol, 2-methoxy-4-methylphenol, isoeugenol, 4-ethylguaiacol, 4-allyl-2,6-dimethoxyphenol (Sigma-Aldrich), ethyl palmitate (Tokyo Chem. Ind.), were used. Phenanthrene was used as an internal standard.

The elemental composition of wood, liquid and solid products of its transformation was determined using an HCNS-O EAFLAS HTM 1112 analyzer (Thermo Quest).

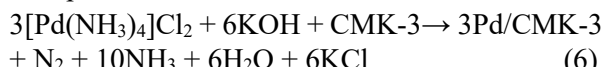
RESULTS AND DISCUSSION

It was previously established³¹ that in an alkaline medium at a temperature of 180 °C, potassium hexachloroiridate(IV) is reduced within 15 minutes by a reaction that can be schematically written as:



Due to the quantitative reduction of potassium hexachloroiridate(IV) by sodium tetrahydridoborate under the specified conditions, it is possible to synthesize materials with a given metal content (Table 1). The slight decrease in the specific surface area of the CMK-3 material is probably due to the contribution of iridium particles, with a significantly lower specific surface area.

Palladium (3% by weight) was applied by decomposing the required amount of tetraamminepalladium (II) at 180 °C in an aqueous solution of potassium hydroxide in the presence of a carbon carrier²³ or the previously synthesized Ir/CMK-3 material. The process proceeds quantitatively with the formation of metallic nanoparticles:



which are uniformly distributed over the surface of the carbon carrier. Table 1 shows the composition and specific surface area of the catalysts.

Electron microscopy studies of the synthesized materials showed (Fig. 1) that spherical particles are formed on the ordered mesoporous carbon support. Palladium particles (Fig. 1a) have a wide size distribution from 3 to 40 nm, and are represented by both individual particles and spherical aggregates. Iridium particles, unlike palladium, have a narrow size distribution with a maximum of 4 nm (Fig. 1b). The material containing two metals is represented by both particles with a maximum at 4 nm, which can be either iridium or palladium, and particles larger than 15 nm, which are most likely metallic palladium (Fig. 1c). Local micro-X-ray fluorescence analysis (Fig. 1d) showed that the Ir-Pd/CMK-3 material consists of C, Pd, and Ir. Platinum metals are distributed fairly evenly over the carrier in a mass ratio close to 1:1, which corresponds to the composition of the sample under the synthesis conditions.

X-ray phase analysis showed (Fig. 2) that, in the range of 2 theta angles from 5 to 80°, there is a peak ($2\Theta = 18^\circ$), probably corresponding to the carbon carrier (2 0 0) and a set of weakly expressed reflections of metals. In the diffraction pattern of the Pd/CMK-3 sample (Fig. 2a) reflections characteristic of palladium appear in the planes (1 1 1), (2 0 0) and (2 2 0) at angles of $2\Theta = 40.2^\circ$, 46.7° and 68.2° , respectively. In the case of the Ir/CMK-3 sample, there are significant broadenings of the lines, which are due to the small size of the crystallites and, probably, microstresses.

Figure 3 shows high-resolution X-ray photoemission spectra of the synthesized Ir/CMK-3 and Pd/CMK-3 materials before and after bombardment with Ar^+ ions for 1 minute. In general, the Ir 4f spectrum (Fig. 3a) can be fitted by at least three components, with the contribution from oxidized ones being initially near to 75%_{at.}, whereas that of the particles after Ar^+ -ion sputtering containing metallic iridium as a dominating form, >50%_{at.} (Fig. 3b).

Table 1
Specific surface area and composition of catalysts on ordered mesoporous carbon CMK-3

Sample	Composition, wt%		Specific area, m^2/g
	Ir%	Pd%	
Ir/CMK-3	3	0	928
Pd/CMK-3	0	3	933
Ir-Pd/CMK-3	2.9	3	908

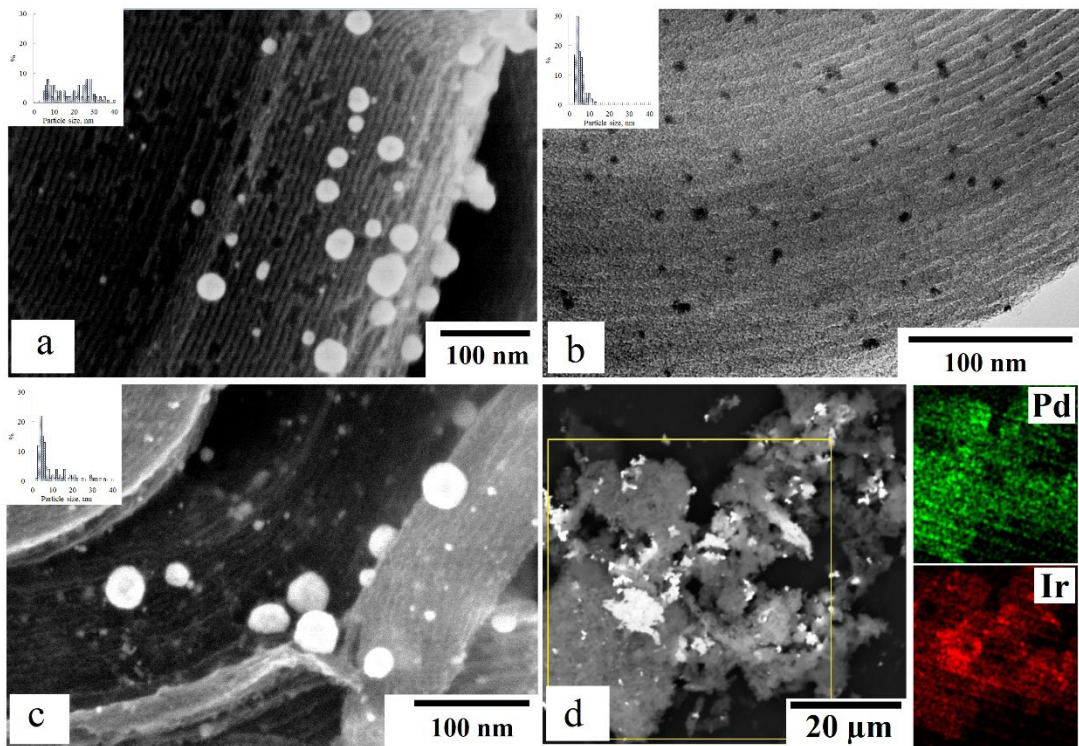


Figure 1: Electron microscopic studies of catalyst samples (inserts show particle size distribution): (a) Pd-CMK-3, high-resolution SEM; (b) Ir-CMK-3, TEM; (c) Ir-Pd-CMK-3, high-resolution SEM; (d) fragment of SEM image and results of Energy-dispersive X-ray Spectroscopy

Due to lack of intensity in the BE region centered at 200 eV (not shown here), which is in accordance with EDS data (not shown here), the absence of Ir-Cl bonding can be concluded. Hence, oxidized Ir species can be attributed to some sort of Ir-O species. The high contribution of Ir-O species is suggested to be related with small nanoparticle sizes in supported state, as compared to bulk metallic powder.^{25,36} The Pd 3d region (Fig. 3c, d) can be fitted by two components with the Pd 3d_{5/2} components centered at BEs of 337.5 eV and 335.9 eV, which are attributable to oxidized Pd(2+)-O species and metallic Pd nanoparticles, correspondingly.³⁷ The spectrum acquired from Pd/CMK-3 sample (Fig. 3c) exhibits ~75%at. Pd(0) species, the contribution of which is decently increased up to >90% after Ar⁺-ion sputtering. Similar regularities are found when analyzing XPS spectra from Ir-Pd/CMK-3 sample.

According to the information provided in Table 2, the use of catalysts helps to reduce the proportion of gaseous products to 1.34 wt%, while the proportion of liquid products increases to 58.6 wt% when using the Pd/CMK catalyst. At the same time, the use of this catalyst causes a decrease in the yield of the solid product to 39.3 wt% compared to the experiment in which the catalyst

was not used (50.0 wt%). The use of the Ir/CMK catalyst gives a yield of the solid product at the level of 45.6 wt%, while the proportion of the liquid product reaches 52.9 wt%, and gaseous products – up to 1.5 wt%. The use of the Pd-Ir/CMK bimetallic catalyst also leads to a decrease in the yield of gaseous products to 1.34 wt%, while the yield of liquid products increases to 58.6 wt%. It is worth noting that the highest conversion is achieved using the Pd/CMK catalyst and is up to 60.7 wt%.

According to the results of chemical analysis presented in Table 3, the use of catalysts in the process of catalytic fractionation of birch wood significantly reduces the level of lignin and hemicelluloses in the solid residue, while increasing the proportion of cellulose. The analysis data confirm that the bimetallic catalyst Pd-Ir/CMK demonstrates higher catalytic activity in the process of hydrogenation of birch wood, which is evident from the decrease in the lignin content in the solid product, reaching 6.0 wt%, and an increase in the proportion of cellulose to 91 wt%. In the process of birch wood fractionation, both in the catalytic and non-catalytic processes, a high degree of hemicellulose conversion (more than 96 wt%) is noted, which is associated with the low

thermal stability of xylan.^{38,39} The use of the Ir-CMK catalyst increases the conversion of lignin by 37.6 wt%, and the use of the Ir-Pd-CMK catalyst

increases this figure by 35.0 wt% compared to the non-catalytic process (Table 4).

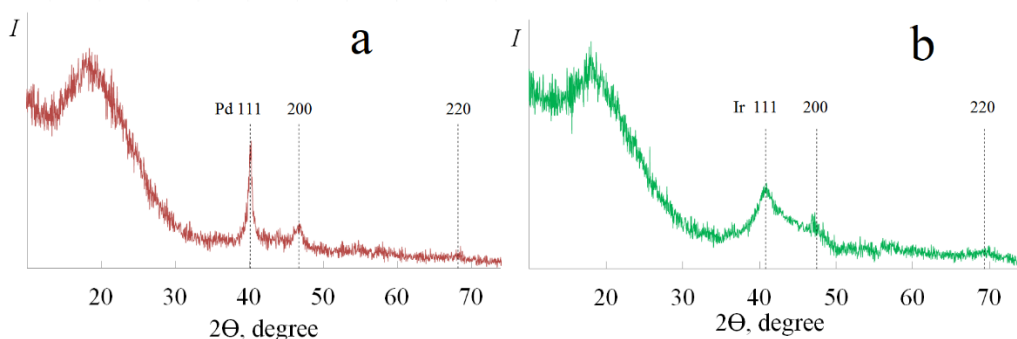


Figure 2: X-ray diffraction patterns of samples: (a) Pd-CMK-3, and (b) Ir-CMK-3

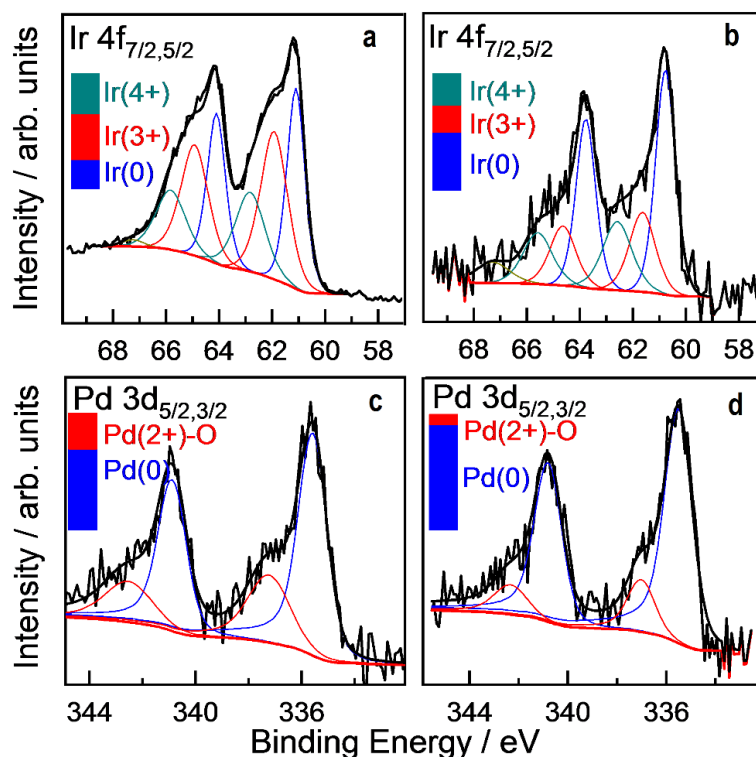


Figure 3: High-resolution X-ray photoelectron spectra before (a,c) and after (b,d) ion bombardment for (a,b) Ir/CMK-3, (c,d) Pd/CMK-3

Table 2
Results of non-catalytic and catalytic hydrogenation of birch wood in supercritical ethanol at 250 °C for 3 hours, $P_{H_2} = 10.0$ MPa

Sample	Conversion, wt%	Yield of liquid products, wt%	Yield of solid products, wt%	Gas yield, mass, %			
				CO	CO ₂	CH ₄	Sum
Without catalyst	50.0	42.4	50.0	3.8	3.1	0.7	7.6
Ir-CMK	54.4	52.9	45.6	0.08	1.4	0.02	1.50
Ir-Pd-CMK	57.2	55.9	42.8	0.1	1.2	0.04	1.34
Pd-CMK	60.7	58.6	39.3	0.3	1.8	0.03	2.13

The Pd-CMK catalyst provides lignin conversion of up to 89.1 wt%. However, it is worth

noting that the use of these catalysts leads to a decrease in cellulose conversion to 3.2 wt%.

Table 3
Chemical composition of solid products of hydrogenation of birch wood samples in supercritical ethanol at 250 °C for 3 hours, $P_{H_2} = 10.0$ MPa

Sample	Composition of solid product, wt%		
	Hemicelluloses	Lignin	Cellulose
Without catalyst	12.5	17.8	69.7
Ir-CMK	3.2	7.0	89.8
Ir-Pd-CMK	3.0	6.0	91.0
Pd-CMK	3.0	6.3	90.7

Table 4
Conversion of structural components of birch wood during hydrogenation in supercritical ethanol at 250 °C

Sample	Cellulose, wt%	Hemicelluloses, wt%	Lignin, wt%
Without catalyst	33.0	82.3	53.6
Ir-CMK	3.2	95.5	91.2
Ir-Pd-CMK	4.2	95.2	88.6
Pd-CMK	13.2	95.4	89.1

Table 5
Composition of gaseous products of hydrogenation of birch wood in supercritical ethanol at 250 °C for 3 hours, $P_{H_2} = 10.0$ MPa

Sample	CO, wt%	CH ₄ , wt%	CO ₂ , wt%
Without catalyst	50.0	9.2	40.8
Ir-CMK	5.5	1.2	93.3
Ir-Pd-CMK	7.5	2.9	89.6
Pd-CMK	14.1	1.4	84.5

As can be seen from the data presented in Table 5, the gaseous products of birch wood hydrogenation mainly consist of carbon monoxide, carbon dioxide and methane. The use of catalysts affects the ratio of these components. This phenomenon was also observed during the hydrogenation of birch wood on palladium-iridium catalysts applied to a taunite carbon substrate.³⁹

The elemental analysis data of the initial birch wood and its hydrogenation products are presented in Table 6. Liquid products obtained as a result of

catalytic hydrogenation of birch wood are characterized by lower oxygen content and higher hydrogen content, compared to the products of non-catalytic hydrogenation. This indicates the occurrence of a process of catalytic hydrodeoxygenation of lignin, as a result of which monomeric and dimeric products are formed.^{40,41} The use of the Ir-Pd-CMK catalyst in the process of reductive fractionation enhances the hydrodeoxygenation processes, reducing the oxygen content to 31.4 wt%.

Table 6
Elemental composition of liquid products of hydrogenation of birch wood samples in supercritical ethanol at 250 °C for 3 hours, $P_{H_2} = 10.0$ MPa

Sample	C, wt%	H, wt%	O, wt%
Initial birch wood	49.8	6.1	44.1
Without catalyst	58.6	7.5	33.9
Ir-CMK	59.8	7.9	32.3
Ir-Pd-CMK	61.0	8.2	31.4
Pd-CMK	59.7	7.1	32.0

Table 7
Yield of monomeric compounds in liquid products of birch wood hydrogenation
in supercritical ethanol at 250 °C

Monomers from the carbohydrate part*	Yield, wt%	Monomers from lignin**
Without catalyst		
1,1-Diethoxyethane	0.71	0.3
Propylene glycol	0.13	0.8
1-Methoxy -butanol-2	0.21	traces
Cyclopentane-1,2-diol	0.52	0.2
Ethyl hexadecanoate	0.19	traces
Acetic acid	0.28	0.1
1-Hydroxybutanone	0.26	0.2
Other monomers, sum	0.13	Less than 0.1
Total	3.14	1.6
Ir-CMK-3		
Furfural	1.01	0.1
Ethyl hexadecanoate	0.43	0.2
2-Furanmethanol	0.21	5.7
1-Hydroxybutanone	1.20	12.8
2-Furanmethanol	0.32	0.1
Tetrahydrofuran-methanol-2	0.38	0.2
Ethyl octadecanoate	0.45	3.8
Ethyl eicanoate	-	0.1
Other monomers, sum	0.80	0.4
Total	4.8	23.4
Ir-Pd-CMK-3		
Furfural	-	0.4
1,1-Diethoxyethane	0.1	0.2
2-Furanmethanol	1.5	0.3
1-Hydroxybutanone	0.3	8.3
2-Furanmethanol		2.7
Tetrahydrofuran-methanol-2	1.4	-
Ethyl octadecanoate	1.3	23.4
Propylene glycol	0.1	4.2
Other monomers, sum	1.1	9.1
Total	5.8	48.6
Pd-CMK-3		
Furfural	-	0.2
Ethyl hexadecanoate	0.1	3.6
2-Furanmethanol	0.5	0.5
1-Hydroxybutanone	0.2	4.2
Propylene glycol	-	1.2
Tetrahydrofuran-methanol-2	0.4	3.2
Ethyl octadecanoate	0.4	31.6
Ethyl eicanoate	0.3	0.4
Other monomers, sum	1.4	4.2
Total	3.6	49.1

* Per weight of liquid fraction of carbohydrate part of products; ** Per weight of Klason lignin

The use of iridium and iridium-palladium catalysts in the process of birch wood hydrogenation in supercritical ethanol leads to an increase in the yields of monomeric substances from the carbohydrate and lignin parts of birch wood biomass (Table 7).

In the presence of iridium and iridium-palladium catalysts, a change in the composition

and yield of monophenolic substances is observed in the process of birch wood hydrogenation. Thus, when using the Ir-CMK-3 catalyst, 4-propenylguaiacol and 4-propylsyringol are observed as the main monophenolic substances with yields of 5.7 and 12.8 wt%, respectively; whereas for the Ir-Pd-CMK and Pd-CMK-3 catalysts, the main monophenolic component is 4-propanolsyringol

with a yield of 23.4 wt% and 31.6 wt%, respectively. Previously, during hydrogenation of birch wood with Ir and Ir-Pd catalysts on the carbon support taunite,³⁹ similar patterns were

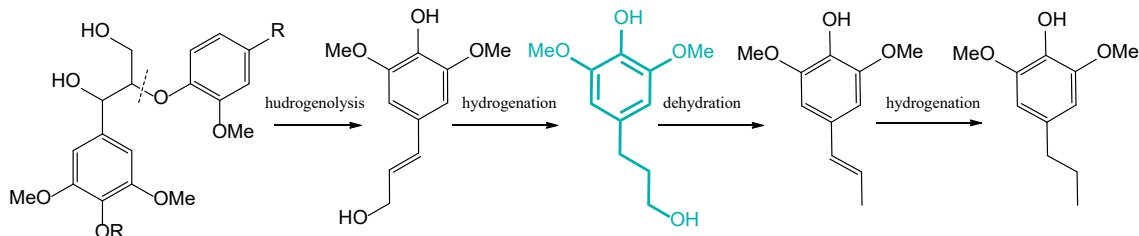


Figure 4: Main products formed during hydrogenation of birch wood in the presence of Ir-Pd-CMK and Pd-CMK-3 catalysts

Among the carbon carriers, the CMK-3 carrier showed the highest activity in the process of hydrogenation of flax shives.⁴² The yield of products increased by almost 1.5 times. This is probably due to the larger specific surface area of CMK-3 and the significantly smaller average grain size of the catalysts compared to catalysts based on Sibunit.

The main products formed during hydrogenation of birch wood in the presence of Ir-Pd-CMK and Pd-CMK-3 catalysts are shown in Figure 4. In the process of reducing catalytic fractionation, wood macromolecules (cellulose, hemicelluloses, lignin) undergo depolymerization on acidic catalyst centers with simultaneous hydrogen stabilization on metal centers. The catalyst accelerates the key reactions of hydrodeoxygenation, hydrogenolysis and hydrogenation, stabilizing the formed fragments and preventing the formation of tar and coke. As a result, complex polymers of wood are transformed into a mixture of hydrocarbons, alcohols, phenols and other oxygen-containing compounds.⁴²

CONCLUSION

Iridium and palladium nanoparticles were obtained on the surface of ordered mesostructured material CMK-3 using a simple hydrothermal method by reducing the corresponding complex compounds. The method of gas adsorption of nitrogen showed that mesoporous carbon has a specific surface area of about 945 m²/g, which slightly decreases after the application of metals. Iridium and palladium particles have a spherical shape and a diameter of 3-40 nm and 2-8 nm, respectively. Micro X-ray fluorescence analysis showed that in the Ir-Pd/CMK-3 sample, the metal particles are uniformly distributed over the surface

obtained, indicating that the Ir catalyst is more selective with respect to 4-propylsyringol.

of the carrier. Using X-ray photoelectron spectroscopy, it was found that iridium is presented in forms (0), (III) and (IV), and palladium in the form of (0) and (II).

The study of the catalytic activity of the synthesized materials in the process of reductive catalytic fractionation (RCF) of birch wood showed that the use of catalysts based on Pd and Pd-Ir significantly increases the yield of liquid products (up to 58.6% by weight) and reduces the lignin content in the solid residue (up to 6.0% by weight). The highest wood conversion (60.7% by weight) was achieved when using the Pd/CMK-3 catalyst. In addition, it was found that the bimetallic catalyst Pd-Ir/CMK-3 demonstrates higher activity in lignin hydrodeoxygenation processes, which is confirmed by a decrease in the oxygen content in liquid products to 31.4% by weight. The results obtained indicate high efficiency of the synthesized catalysts for the processing of lignocellulosic biomass into valuable chemical products, such as monomeric phenolic compounds and carbohydrates. This opens up new prospects for the development of sustainable biomass processing technologies with minimal energy consumption and waste. Further research can be aimed at optimizing the catalyst composition and process conditions to increase selectivity and yield of target products.

ACKNOWLEDGMENTS: The work was carried out within the framework of the state assignment of the Institute of Chemistry and Chemical Technology SB RAS (project No. FWES-2021-0014) using the equipment of the Krasnoyarsk Regional Center for Collective Use of the Federal Research Center KSC SB RAS.

REFERENCES

- ¹ B. Huang and Y. Zhao, *EcoMat*, **2022**, e12176 (2022), <https://doi.org/10.1002/eom2.12176>
- ² H. Li, Y. Lin, J. Duan, Q. Wen, Y. Liu *et al.*, *Chem. Soc. Rev.*, **53**, 10709 (2024), <https://doi.org/10.1039/D3CS00010A>
- ³ F. Lv, J. Feng, K. Wang, Z. Dou, W. Zhang *et al.*, *ACS Cent. Sci.*, **4**, 1244 (2018), <https://doi.org/10.1021/acscentsci.8b00426>
- ⁴ H. Over, *ACS Catal.*, **11**, 8848 (2021), <https://doi.org/10.1021/acscatal.1c01973>
- ⁵ F. Wang, K. Kusada, D. Wu, T. Yamamoto, T. Toriyama *et al.*, *Angew. Chem. Int. Ed.*, **57**, 4505 (2018), <https://doi.org/10.1002/anie.201800650>
- ⁶ D. Liu, X. Chen, G. Xu, J. Guan, Q. Cao *et al.*, *Sci. Rep.*, **6**, 21365 (2016), <https://doi.org/10.1038/srep21365>
- ⁷ L. M. Martínez-Prieto, I. Cano and P. W. van Leeuwen, in “Iridium Catalysts for Organic Reactions. Topics in Organometallic Chemistry”, edited by L. A. Oro and C. Claver, Springer, Cham, 2021, vol. 69, p. 397, https://doi.org/10.1007/3418_2020_60
- ⁸ X. Kang, Y. Li, M. Zhu and R. Jin, *Chem. Soc. Rev.*, **49**, 6443 (2020), <https://doi.org/10.1039/C9CS00633H>
- ⁹ T. S. Rodrigues, A. G. da Silva and P. H. Camargo, *J. Mater. Chem. A*, **7**, 5857 (2019), <https://doi.org/10.1039/C9TA00074G>
- ¹⁰ F. Sanchez, L. Bocelli, D. Motta, A. Villa, S. Albonetti *et al.*, *Appl. Sci.*, **10**, 1752 (2020), <https://doi.org/10.3390/app10051752>
- ¹¹ K. D. Gilroy, A. Ruditskiy, H. Peng, D. Qin and Y. Xia, *Chem. Rev.*, **116**, 10414 (2016), <https://doi.org/10.1021/acs.chemrev.6b00211>
- ¹² H. Luo, F. Lin, Q. Zhang, D. Wang, K. Wang *et al.*, *J. Am. Chem. Soc.*, **146**, 19327 (2024), <https://doi.org/10.1021/jacs.4c05165>
- ¹³ L. A. Putri, Y. D. Prabowo, D. M. M. Dewi, Z. Mumtazah, F. P. Adila *et al.*, *ACS Appl. Nano Mater.*, **7**, 19821 (2024), <https://doi.org/10.1021/acsanm.4c04327>
- ¹⁴ A. Chen and C. Ostrom, *Chem. Rev.*, **115**, 11999 (2015), <https://doi.org/10.1021/acs.chemrev.5b00324>
- ¹⁵ M. Hara, R. Badam, G. J. Wang, H. H. Huang and M. Yoshimura, *ECS Trans.*, **85**, 27 (2018), <https://doi.org/10.1149/08511.0027ecst>
- ¹⁶ H. Bernas, I. Simakova, I. P. Prosvirin, P. Mäki-Arvela, R. Leino *et al.*, *Catal. Lett.*, **142**, 690 (2012), <https://doi.org/10.1007/s10562-012-0809-1>
- ¹⁷ O. V. Belousov, V. E. Tarabanko, R. V. Borisov, I. L. Simakova, A. M. Zhyzhaev *et al.*, *React. Kinet. Mech. Catal.*, **127**, 25 (2019), <https://doi.org/10.1007/s11144-018-1430-0>
- ¹⁸ Z. Wang, W. Chen, Z. Han, J. Zhu, N. Lu *et al.*, *Nano Res.*, **7**, 1254 (2014), <https://doi.org/10.1007/s12274-014-0488-x>
- ¹⁹ S. Shinae, S. H. Joo, R. Ryoo, M. Kruk, M. Jaroniec *et al.*, *J. Am. Chem. Soc.*, **122**, 10712 (2000), <https://doi.org/10.1021/ja002261e>
- ²⁰ I. V. Ponomarenko, V. A. Parfenov, Y. N. Zaitseva, S. D. Kirik and S. M. Zharkov, *Glass Phys. Chem.*, **40**, 79 (2014), <https://doi.org/10.1134/S1087659614010180>
- ²¹ L. A. Solovyov, *Chem. Soc. Rev.*, **42**, 3708 (2013), <https://doi.org/10.1039/C3CS60003E>
- ²² X. Xia, S. Xie, M. Liu, H. C. Peng, N. Lu *et al.*, *Proc. Natl. Acad. Sci. U.S.A.*, **110**, 6669 (2013), <https://doi.org/10.1073/pnas.1222109110>
- ²³ R. V. Borisov, O. V. Belousov and A. M. Zhyzhaev, *Russ. J. Inorg. Chem.*, **65**, 1623 (2020), <https://doi.org/10.1134/S0036023620100034>
- ²⁴ R. V. Borisov, O. V. Belousov, A. M. Zhyzhaev, M. N. Likhatski and N. V. Belousova, *Russ. Chem. Bull.*, **70**, 1474 (2021), <https://doi.org/10.1007/s11172-021-3242-z>
- ²⁵ R. V. Borisov, O. V. Belousov, A. M. Zhyzhaev, S. D. Kirik and Y. L. Mikhlin, *Inorg. Mater.*, **58**, 131 (2022), <https://doi.org/10.1134/S0020168522020030>
- ²⁶ M. Jindal, P. Uniyal and B. Thallada, *Bioresour. Technol.*, **385**, 129396 (2023), <https://doi.org/10.1016/j.biortech.2023.129396>
- ²⁷ X. Li, Y. Xu, K. Alorku, J. Wang and L. Ma, *Mol. Catal.*, **550**, 113551 (2023), <https://doi.org/10.1016/j.mcat.2023.113551>
- ²⁸ W. Arts, K. Van Aelst, E. Cooreman, J. Van Aelst, S. Van den Bosch *et al.*, *Energ. Environ. Sci.*, **16**, 2518 (2023), <https://doi.org/10.1039/D3EE00965C>
- ²⁹ S. Qiu, M. Wang, Y. Fang and T. Tan, *Sustain. Energ. Fuels*, **4**, 5588 (2020), <https://doi.org/10.1039/D0SE01118E>
- ³⁰ T. Renders, G. Van den Bossche, T. Vangeel, K. Van Aelst and B. Sels, *Curr. Opin. Biotechnol.*, **56**, 193 (2019), <https://doi.org/10.1016/j.copbio.2018.12.005>
- ³¹ R. V. Borisov, O. V. Belousov, M. N. Likhatski, A. M. Zhyzhaev and S. D. Kirik, *Russ. Chem. Bull.*, **71**, 1164 (2022), <https://doi.org/10.1007/s11172-022-3517-z>
- ³² Y. L. Mikhlin, R. V. Borisov, S. A. Vorobyev, Y. V. Tomashевич, A. S. Romanchenko *et al.*, *J. Mater. Chem. A*, **10**, 9621 (2022), <https://doi.org/10.1039/D2TA00877G>
- ³³ A. I. Ruiz-Matute, M. L. Sanz and I. Martínez-Castro, *J. Chromatogr. B*, **879**, 1226 (2011), <https://doi.org/10.1016/j.jchromb.2010.11.013>
- ³⁴ A. V. Obolenskaya and Z. P. Elnitskaya, “Laboratory Work on the Chemistry of Wood and Cellulose”, Ecology, Moscow, 1991
- ³⁵ E. Sjöström and R. Alén, “Analytical Methods in Wood Chemistry, Pulping, and Papermaking”, Springer-Verlag, Berlin-Heidelberg, 1999
- ³⁶ F. Claudel, L. Dubau, G. Berthomé, L. Solà-Hernández, C. Beauger *et al.*, *ACS Catal.*, **9**, 4688 (2019), <https://doi.org/10.1021/acscatal.9b00280>
- ³⁷ A. Felten, J. Ghijssen, J.-J. Pireaux, W. Drube, R. L. Johnson *et al.*, *Micron*, **40**, 74 (2009), <https://doi.org/10.1016/j.micron.2008.01.013>

³⁸ D. M. Carvalho, J. L. Colodette, M. Martínez and A. R. Gonçalves, *Carbohyd. Polym.*, **220**, 132 (2019), <https://doi.org/10.1016/j.carbpol.2019.05.074>

³⁹ A. S. Kazachenko, R. V. Borisov, A. V. Miroshnikova, O. S. Selezneva, A. M. Skripnikov *et al.*, *J. Sib. Fed. Univ. Chem.*, **17**, 505 (2024)

⁴⁰ A. V. Miroshnikova, A. S. Kazachenko, V. E. Tarabanko and O. P. Taran, *Catal. Ind.*, **14**, 231 (2022), <https://doi.org/10.1134/S2070050422020065>

⁴¹ W. Schutyser, T. Renders, S. Van den Bosch, S.-F. Koelewijn, G. T. Beckham *et al.*, *Chem. Soc. Rev.*, **47**, 852 (2018), <https://doi.org/10.1039/C7CS00566K>

⁴² A. V. Miroshnikova, V. V. Sychev, V. E. Tarabanko, A. S. Kazachenko, A. M. Skripnikov *et al.*, *Int. J. Mol. Sci.*, **24**, 11709 (2023), <https://doi.org/10.3390/ijms241411709>